Vol. 132: 171–179, 2019
https://doi.org/10.3354/dao03317

DISEASES OF AQUATIC ORGANISMS
Dis Aquat Org

Published online January 24

Morphological and molecular characterization of the muscle-infecting myxosporean *Myxobolus xinyangensis* sp. nov. from *Abbottina rivularis* in China

W. Wu[1,2,*], Q. S. Wang[1,*], H. Sato[3], J. Y. Zhang[1,2,3,]**

[1]Key Laboratory of Aquaculture Diseases Control, Ministry of Agriculture, State Key Laboratory of Freshwater Ecology and Biotechnology, HuaiAn Research Center, Institute of Hydrobiology, Chinese Academy of Sciences, Wuhan, 430072, PR China
[2]University of Chinese Academy of Sciences, Beijing, 100049, PR China
[3]Laboratory of Parasitology, Joint Faculty of Veterinary Medicine, Yamaguchi University, Yamaguchi, 753-8515, Japan

ABSTRACT: During an environmental assessment on the Huang River in Xinyang City (Henan Province, China), a novel *Myxobolus* species (Myxozoa: Myxobolidae) was found infecting the trunk muscle of Chinese false gudgeon *Abbottina rivularis* Basilewsky, 1855 (Gobioninae, Cyprinidae). Plasmodia of the new myxozoan, nominated herein as *Myxobolus xinyangensis* sp. nov., are round and yellowish, symmetrically and bilaterally located dorsal to the openings of the 2 opercula, and measure about 4.5 mm in diameter. The mature myxospores are orbicular in frontal view and fusiform in sutural view, with slightly tapered anterior end and rounded posterior end, and measure 9.4 ± 0.5 (8.7–10.6) µm long, 8.6 ± 0.6 (7.3–9.5) µm wide and 6.4 ± 0.3 (5.8–7.1) µm thick (mean ± SD, range). The ratio of spore length to spore width is close to 1. Two slightly unequal pyriform polar capsules, with tapering anterior ends and rounded posterior ends, measure 5.6 ± 0.67 (4.3–6.8) µm long and 3.0 ± 0.3 (2.4–3.6) µm wide, present as a figure 8 in the anterior part of spores and tightly converge at the top end of spores. Polar filament coils show 4 to 5 turns and are situated perpendicularly to the longitudinal axis of the polar capsules. No intercapsular appendix or sutural folds at the posterior end of spores were observed. The obtained partial small subunit ribosomal DNA sequence did not match any available data in GenBank and showed the highest sequence identity (93%) with 2 cyprinid trunk muscle-infecting *Myxobolus* species, *M. pseudodispar* and *M. klamathellus*. Phylogenetic analysis clearly showed that *M. xinyangensis* sp. nov. clustered within a cyprinid trunk muscle-infecting *Myxobolus* subclade at the basal position, but as an independent branch which was a possible reflection of its distinct myxospore morphology. This is the first record of infection of *Myxobolus* species in the trunk muscle of *Abbotina* fish.

KEY WORDS: Chinese false gudgeon · Myxozoa · Trunk muscle · Morphology · Phylogeny

1. INTRODUCTION

Chinese false gudgeon *Abbottina rivularis* Basilewsky (Cypriniformes: Cyprinidae) is a widely distributed small freshwater cyprinid in East Asia, which is native to eastern China and the Korean Peninsula and was introduced to southeastern and central Asia (Hayashi et al. 2013). *A. rivularis* naturally inhabits shallow zones of lentic rivers, ponds and lakes with sandy or muddy bottoms, which may provide suitable conditions for infections with myxosporeans. To date, 28 nominal myxosporean species

*These authors contributed equally to this work
**Corresponding author: zhangjy@ihb.ac.cn

have been recorded in *A. rivularis* and its 2 congeners in China, including 2 *Chloromyxum* species, 3 *Zschokkella* species, 5 *Myxidium* species and 18 *Myxobolus* species (Chen & Ma 1998, Eiras et al. 2005). However, the original descriptions of some of these species were incomplete and based solely on myxospore morphology and thus these species warrant further evidence to validate them. Records of multi-hosts or multi-infection sites for a given species are frequent in the monograph of Chen & Ma (1998). Among the *Myxobolus* species reported to infect *Abbottina* spp., *M. chuhsienensis*, *M. haichengensis*, *M. kiatingensis*, *M. mapienensis*, *M. pseudodisparoides*, *M. schirzothoraxi* and *M. abbottinae* were originally documented as new species based on morphological and morphometric data (Chen & Ma 1998). However, only *M. haichengensis* was recently proven to be a valid species by a holistic taxonomic approach combining myxospore morphology, tissue tropism, host biology and molecular data (Li et al. 2018). To validate the nominated myxosporeans infecting *Abbottina* spp. in China and further uncover their true diversity, a joint project was initiated between ichthyologists and fish ecologists of the Institute of Hydrobiology (Chinese Academy of Sciences). As a part of this ongoing project, a novel species, *Myxobolus xinyangensis* sp. nov., is described herein with robust morphological and molecular characteristics, which formed distinct connected cysts in the trunk muscle of *A. rivularis* collected from the Huang River in Xinyang City, Henan Province, China. This is the first report of a trunk muscle-dwelling myxosporean in *A. rivularis*.

2. MATERIALS AND METHODS

2.1. Sample collection and morphological observations

Fish specimens were captured by ground net cages in November 2017 from the Guangshan County reach of the Huang River (Xinyang City, Henan Province, China; 31° 84′ 41″ N, 115° 00′ 64″ E), a main upstream tributary of the Huai River, which is one of the 7 largest rivers in China. Suspected myxozoan plasmodia were screened by eye when investigating the fish resource and population structure required for environmental assessment. Fish specimens with suspected plasmodia were preserved in 95% ethanol and transported to the laboratory of the Institute of Hydrobiology, Chinese Academy of Sciences, for further species identification. The suspected plasmodia were isolated from the preserved fish and washed several times with distilled water. After rinsing in distilled water for 12 h at room temperature, the plasmodia were ruptured by a fine needle to make wet preparations for morphological characterization. The remaining plasmodia were subjected to the following molecular characterization. Wet mounts were observed under an oil immersion objective (1000×) with an Olympus BX 53 microscope equipped with an ocular micrometer. Mature myxospores were photographed with Zeiss Axioplan 2 Image and Axiophot 2. Line drawings were made based on the photographs with the aid of Adobe Photoshop CS (Adobe Systems). Iodinophilous vacuoles and mucus envelopes of the spores could not be observed in fixed specimens. Morphological and morphometric data of 30 randomly selected mature myxospores were obtained according to Lom & Arthur (1989). All measurements are given in µm as mean ± SD, followed by the range in parentheses, unless otherwise stated. The presence of possible myxosporean plasmodia in gills, skin, kidney, gallbladder, heart, spleen and intestinal contents was also roughly determined by eye and by examining wet mounts under light microscopy after necropsy.

2.2. Genomic DNA extraction and sequencing

Ethanol-preserved plasmodia contents were washed 2 times with distilled water to remove the ethanol remnants. Genomic DNA (gDNA) of the novel myxosporean was extracted using the Qiagen DNeasy Blood & Tissue Kit as per the manufacturer's recommended protocol for animal tissue. The obtained gDNA concentration was determined with a NanoDrop 2000 spectrophotometer (Thermo Fisher Scientific) at 260 nm. The partial sequence of the small subunit ribosomal DNA (SSU rDNA) gene was amplified using the primer pair MyxospecF/18R, with an expected amplicon of about 1600 bp (Whipps et al. 2003, Fiala 2006). PCR was performed in a 25 µl reaction volume, comprising about 30 ng template DNA, 1×PCR mixture (CWbiotech) and 10 pmol of each primer pair. Cycling conditions consisted of an initial denaturation step at 95°C for 4 min, followed by 35 cycles at 95°C for 1 min, 48°C for 1 min, 72°C for 2 min, and a final extension of 7 min at 68°C. The obtained PCR amplicons were visualized by 1% agarose gel electrophoresis with SYBR safe DNA gel stain (Thermo Fisher Scientific) under ultraviolet light, purified with a PCR purification kit (CWbiotech), and then cloned into a PMD-18 T vector system

(Takara). Three randomly selected positive clones were sequenced in both directions using vector primers (M13/M47) with the ABI DigDye Terminator v3.1 Cycle Sequencing Kit with an ABI 3100 Genetic Analyzer.

2.3. Phylogenetic analysis

All sequences were assembled using BioEdit (Hall 1999), and the consensus sequences obtained were determined to be myxozoan by a GenBank BLAST search. To explore the phylogenetic position of the present species, sequences with high search scores and those of representative *Myxobolus* species with plasmodia located intracellularly in muscle of cyprinid fish were retrieved from GenBank. In total, 30 sequences were aligned with Clustal X (Thompson et al. 1997) using the default settings. The alignment was corrected manually with the alignment editor of the software MEGA 6.0 (Tamura et al. 2013) by eliminating positions containing gaps and missing data. DNA pairwise sequence distance estimation was performed using the Kimura-2-parameter model distance matrix for transitions and transversions. Phylogenetic analysis of the final aligned dataset was conducted using maximum likelihood (ML) in PhyML 3.0 and Bayesian inference (BI) in Mr. Bayes (Ronquist & Huelsenbeck 2003, Guindon et al. 2010). The optimal nucleotide substitution model of the best fit for ML and BI was determined by jModelTest 3.07 (Posada 2008) to be GTR+I+G based on the highest value of the corrected Akaike's information criterion. *Ceratonova shasta* (AF001579) was used as the outgroup to root the tree. Two independent runs were conducted with 4 chains for 1 million generations for BI. Phylogenetic trees were sampled every 100 generations. The first 25% of the samples were discarded from the cold chain (burninfrac = 0.25). Bootstrap confidence values were calculated with 100 pseudoreplicates for ML. Support values below 50 are not shown. The tree was initially examined in TreeView (Page 1996) and then edited and annotated in Adobe Illustrator (Adobe Systems).

3. RESULTS

In total, 24 fish species were collected, all of which were identified to species by the ichthyologists involved in the project (see Table A1 in the Appendix). The prevalence of myxosporean infection was only determined based on the presence of plasmodia observed by eye. One out of 51 *Abbottina rivularis* (prevalence of 1.96%) with average body weight of 10.2 g and body length of 7.7 cm was found to be infected by a suspected myxosporean. Five plasmodia were located bilaterally dorsal to the 2 opercular openings, with 2 and 3 connected plasmodia located in the left and right side of the operculum, respectively. The plasmodia were round and yellowish, measuring about 4.5 mm in diameter (Fig. 1). We found no other infection site in *A. rivularis* and no infection by this unidentified myxosporean in any of the other captured sympatric fish.

3.1. Species description and morphological comparisons

The myxospores are typical of *Myxobolus*. Mature myxospores are orbicular in frontal view and fusiform in sutural view, with a slightly tapered anterior end and round posterior end, and measure 9.4 ± 0.5 (8.7–10.6) µm long, 8.6 ± 0.6 (7.3–9.5) µm wide and 6.4 ± 0.3 (5.8–7.1) µm thick. Spore valves are thin and symmetrical, with smooth surfaces. The sutural ridge is straight and thick, but does not protrude out of the spore ends. The ratio of spore length to width is about 1. Two pyriform polar capsules are slightly unequal, presenting as a figure 8 in the anterior part of the spore, measure 5.6 ± 0.67 (4.3–6.8) µm long and 3.0 ± 0.3 (2.4–3.6) µm wide and tightly converge at the top end of the spore, with a tapering anterior end and a round posterior end. The length of the polar capsules is more than half of the spore length. Polar filaments coil with 4–5 turns and are situated perpendicularly to the longitudinal axis of the polar capsules. No intercapsular appendix or sutural markings at the posterior end of spore were observed (Figs. 2 & 3).

Among 18 nominated *Abbottina*-infecting *Myxobolus* species, *M. physophilus*, *M. obovoides*, *M. obliquus* and *M. pseudosquamae* are morphologi-

Fig. 1. Plasmodia of *Myxobolus xinyangensis* sp. nov. symmetrically located in the dorsal trunk muscle on the back side of the operculum of *Abbotina rivularis*, with 2 and 3 fused plasmodia on the left and right side of the host body, respectively

Fig. 2. Mature myxospores of *Myxobolus xinyangensis* sp. nov. in (a) sutural and (b) frontal view

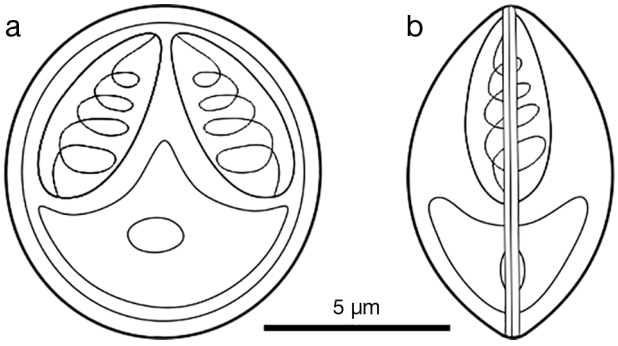

Fig. 3. Schematic drawing of myxospores of *Myxobolus xinyangensis* sp. nov. from *Abbotina rivularis*, in (a) frontal view and (b) sutural view

cally superficially similar to the present species, as they all have a round or ovoid myxospore morphology. However, *M. physophilus* and *M. obovoides* are distinct from *M. xinyangensis* sp. nov. by their larger spore body and more coils of the polar filament (6–7 and 7–8, respectively vs. 4–5). Furthermore, the anterior end of the spore of *M. physophilus* is sharp, rather than orbicular, as in *M. xinyangensis* sp. nov. *M. obliquus* can be distinguished from *M. xinyangensis* sp. nov. by having smaller spore body and narrower spore posterior end. The ratio of spore length to spore width of *M. pseudosquamae* is significantly larger than that of *M. xinyangensis* sp. nov., and the 2 polar capsules of *M. pseudosquamae* do not converge as tightly as those of the present species. More importantly, *M. xinyangensis* sp. nov. is the only species reported to date that infects trunk muscles of *Abbottina* spp. (Table 1). Further morphological comparisons with other nominated species that infect muscles of cyprinids and have round spore bodies showed that the novel species was superficially similar to *M. yibenensis* and *M. artus*, which are both *Cyprinus carpio*-infecting species; however, the spore length of the latter 2 species is shorter than their spore width. The oblate spore body of *M. yibenensis* and *M. artus* was remarkably different from the orbicular spore body of the present species (Ogawa et al. 1992, Chen & Ma 1998). *M. stanlii* is distinctly different from *M. xinyangensis* sp. nov. in that it has thick spore valves, polar capsules of equal size and more polar filament coils (5–7 vs. 4–5) (Iwanowicz et al. 2013). An unidentified muscle-infecting *Myxobolus* species associated with vertebral deformities in cyprinid fish in the USA is morphologically similar to *M. cyprini* (Kent et al. 2004), which can also be morphologically distinguished from the present species.

Table 1. Morphological comparisons of *Myxobolus xinyangensis* sp. nov. with other *Abbottina*-infecting species with round or ovoid spore body. IF: infection site; SBS: spore body shape; SL: spore length; SW: spore width; ST: spore thickness; PCL: length of polar capsule; PCW: width of polar capsule; PFC: number of polar filament coils. Values in the first row are given as means ± SD; ranges are in parentheses

Myxobolus species	IF	SBS	SL (µm)	SW (µm)	ST (µm)	PCL (µm)	PCW (µm)	PFC
M. xinyangensis sp. nov.	Muscle	Round	9.4 ± 0.45 (8.7–10.6)	8.6 ± 0.61 (7.3–9.5)	6.4 ± 0.28 (5.8–7.1)	5.6 ± 0.67 (4.3–6.8)	3.0 ± 0.27 (2.4–3.6)	4–5
M. physophilus	Gill	Ovoid	12.5 (12.0–13.0)	9.0 (8.4–9.6)	8.4	7.2 (6.6–8.4)	3.1 (2.8–3.6)	6–7
M. obovoides	Gill/kidney	Round	14.2 (13.8–14.4)	13.5 (13.2–14.4)	8.4	7.7 (7.2–8.0)	5.8 (5.4–6.0)	7–8
M. obliquus	Kidney	Ovoid	8.4 (7.8–9.0)	8.1 (7.2–8.4)	6.2 (6.0–7.2)	4.0 (3.8–4.2)	2.5 (2.4–2.6)	4–5
M. pseudosquamae	Gill	Ovoid	11.46 (11.2–12.0)	8.53 (8.0–8.8)	6.13 (6.0–6.4)	5.6	3.06 (2.8–3.2)	?

3.2. Molecular characteristics

The sequences of 3 clones were 100% identical to one another. A final consensus sequence of 1720 bp of SSU rDNA with 45.52% GC content was successfully obtained after trimming the ambiguous parts and primer sequences and was deposited in GenBank under accession number AF001579. A sequence similarity search by nucleotide BLAST clearly revealed that it did not match any sequences available in GenBank, but presented relatively high sequence similarity with several *Myxobolus* species infecting muscle of cyprinid fish. Sequence comparisons showed that the present species was most closely related to *M. pseudodispar* (93.2%, KU340983), *M. klamathellus* (93.2%, KX261616), *M. musculi* (93.1%, JQ388891), *M. artus* (92.8%, FJ710799), *M. cyprini* (92.6%, AF380140), *M. bhadrensis* (91.9%, KM029971), *M. kingchowensis* (91.7%, KP400625), *M. stanlii* (91.7%, DQ779995), *Myxobolus* sp. (91.5%, AY591531), *M. terengganuensis* (91.2%, EU643629) and *M. ladogensis* (90.9%, KU160629), all of which intracellularly infect the muscle of cyprinid fish. However, the novel species was genetically distant from *M. haichengensis*, a species infecting the gill filaments of *A. rivularis* in China (Table 2). Phylogenetic analysis also clearly revealed that this novel species clustered with *M. bhadrensis, M. kingchowensis* and *M. terengganuensis* to form an independent subclade which was positioned within the clade of *Myxobolus* spp. that infect cyprinids intra-muscularly (Fig. 4).

3.3. Taxonomic summary of *Myxobolus xinyangensis* sp. nov.

Type host: *Abbottina rivularis* Basilewsky (Cypriniformes: Cyprinidae).
Type locality: Huang River, Xinyang City, Henan Province, China (31° 84′ 41″ N, 115° 00′ 64″ E).
Infection site: Trunk muscle.
Type material: Digitized photos of syntype myxospores and 70% ethanol-preserved plasmodia were deposited in the Laboratory of Fish Diseases, Institute of Hydrobiology, Chinese Academy of Sciences, under accession number MTR20171206. The partial 18S rDNA was deposited in GenBank under accession number AF001579.
Prevalence: 1 of 51 (1.96%).
Etymology: The species is named after the type locality, Xinyang City, China.

4. DISCUSSION

Myxobolus Bütschli, 1882 is the most speciose genus among the phylum Myxozoa, with more than 900 nominated species (Eiras et al. 2005, 2014), and the number of described species is continuously increasing (Atkinson & Banner 2017, Guo et al. 2018). However, many nominated species have been described solely based on simple myxospore morphological data, and some only with line drawings, especially for species recorded in China, Russia and India (Chen & Ma 1998, Liu et al. 2016). An integrative taxonomic approach of combining myxospore mor-

Table 2. Pairwise nucleotide sequence identity percentage (above diagonal) and DNA distance using Kimura 2-parameter model (below diagonal) among *Myxobolus xinyangensis* sp. nov. and cyprind-infecting *Myxobolus* species with high sequence similarity

Myxobolus species	Table ID	1	2	3	4	5	6	7	8	9	10	11	12	13
M. xinyangensis sp. nov.	1	–	93.2	93.2	93.1	92.8	92.6	91.9	91.7	91.7	91.5	91.2	90.9	70.6
M. pseudodispar	2	0.068	–	96.1	95.1	95.3	95.6	94.1	93.1	94.6	95.7	93.7	95.0	72.3
M. klamathellus	3	0.068	0.039	–	96.2	93.9	94.3	93.5	92.2	94.3	95.6	92.2	94.6	72.4
M. musculi	4	0.069	0.049	0.038	–	93.8	94.3	93.8	93.0	95.4	96.5	92.5	95.4	72.1
M. artus	5	0.072	0.047	0.061	0.062	–	99.2	93.2	92.7	92.7	93.9	92.1	93.0	72.0
M. cyprini	6	0.074	0.044	0.057	0.057	0.008	–	93.7	93.2	93.0	94.2	92.5	93.3	72.6
M. bhadrensis	7	0.081	0.059	0.065	0.062	0.068	0.063	–	94.1	91.9	92.9	94.4	92.4	72.7
M. kingchowensis	8	0.083	0.069	0.072	0.070	0.073	0.068	0.059	–	91.7	91.7	94.1	91.0	72.4
M. stanlii	9	0.083	0.054	0.057	0.046	0.073	0.070	0.081	0.083	–	94.7	91.5	93.2	71.7
Myxobolus sp.[a]	10	0.085	0.043	0.044	0.035	0.061	0.058	0.071	0.083	0.053	–	92.8	95.3	72.2
M. terengganuensis	11	0.088	0.063	0.078	0.075	0.079	0.075	0.056	0.059	0.085	0.072	–	92.1	71.4
M. ladogensis	12	0.091	0.050	0.054	0.046	0.070	0.067	0.076	0.090	0.068	0.047	0.079	–	70.5
M. haichengensis	13	0.294	0.277	0.276	0.279	0.280	0.274	0.273	0.276	0.283	0.278	0.286	0.295	–

[a]An unnamed *Myxobolus* species from skeletal muscles of *Ptychocheilus oregonensis* (Cyprinidae) (GenBank accession number AY591531)

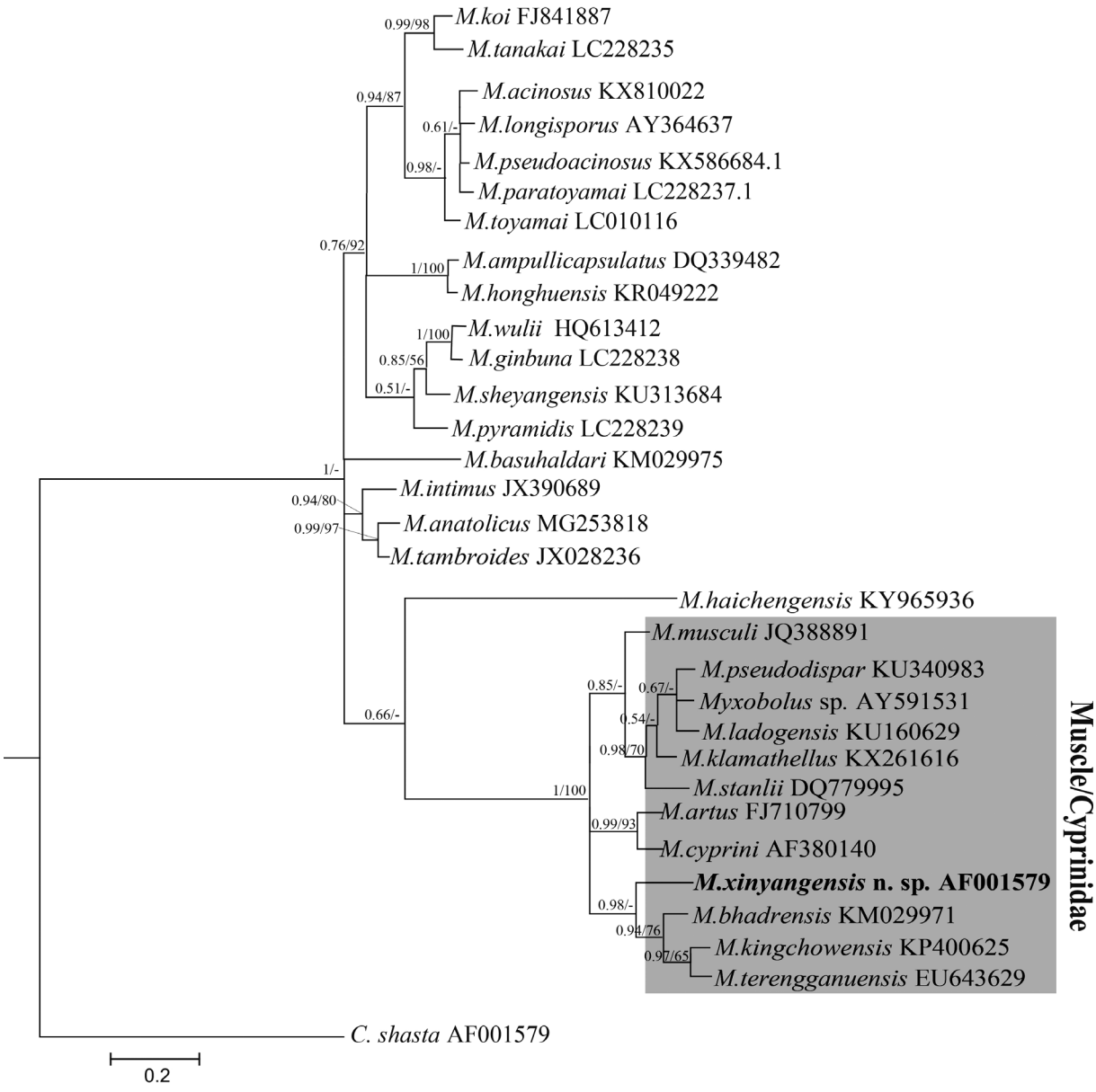

Fig. 4. Phylogenetic tree generated by Bayesian analysis (BI) and maximum likelihood (ML) of the aligned partial SSU rRNA gene sequences of *Myxobolus xinyangensis* sp. nov. and related cyprinid-infecting congeners, rooted at *Cernotova shasta*. GenBank accession numbers are given adjacent to the corresponding species name. Numbers at nodes indicate posterior probabilities of BI and bootstrap support values of ML, respectively. Dashes represent values under 50%. The new species is highlighted in **bold** and the cyprinid muscle-infecting cluster is shaded

phology, ecological features (host affinity, tissue tropism and geographical distribution) and molecular characteristics has been widely accepted for species descriptions of myxosporeans and identification of possible cryptic species (Atkinson et al. 2015), for descriptions of extensive intraspecific morphological variations (Zhai et al. 2015, Guo et al. 2018) and for descriptions of interspecific morphological similarity among this group of ubiquitous parasites (Zhang et al. 2010). Although several evolutionary pressures have been suggested to drive the speciation of myxosporeans, it remains enigmatic how these taxonomic characteristics evolved during their radiation history (Bartošová et al. 2009, Fiala et al. 2015). One reason for the uncertainty lies in the lack of sufficient data as a result of under-sampling; therefore, one of the main tasks for ichthyo-parasitologists is to apply this integrative approach to validate the nominated species that have incomplete descriptions and to describe novel taxa.

In the present study, we have described a novel trunk muscle-infecting *Myxobolus* species, designated as *M. xinyangensis* sp. nov., based on robust morphological, ecological and molecular characteristics. This species was obtained from wild *A. rivularis* caught during an environmental assessment of an upstream tributary of the Huai River in China. Given the lack of sufficient funding support for most ichthyo-parasitologists worldwide, we think that cooperating with other agencies or individuals is a feasible way to increase sampling efforts and thus better describe the diversity of fish myxozoan parasites. No myxosporean infections in *A. rivularis* have been found outside of China (Chen & Ma 1998, Eiras et al. 2005, 2014), although this small cyprinid has a wide distribution throughout East Asia. Based on strict morphological comparisons, we determined that *M. xinyangensis* sp. nov. is significantly different from all known *Abbottina*-infecting and cyprinid muscle-infecting congeners. The partial SSU rDNA sequence of *M. xinyangensis* sp. nov. is 93.2% identical to that of *M. pseudodispar* and *M. klamathellus*, which is the highest identity among available data in GenBank. All species with high sequence similarity with *M. xinyangensis* sp. nov. infect the muscle of cyprinids; however, they can be discriminated from *M. xinyangensis* sp. nov. by significant morphological discrepancies, especially their elongated oval spore bodies (*M. bhadrensis*, *M. terengganuensis*, *M. kingchowensis*, *M. klamathellus* and *M. ladogensis*) (Székely et al. 2009, 2015, Zhao et al. 2017) and polar capsules of distinct unequal size (*M. cyprini*, *M. musculi* and *M. pesudodispar*) (Molnár et al. 2002, Forró & Eszterbauer 2016).

Molecular phylogenetic analysis of *Myxobolus* species involved in cyprinid intramuscular infection clearly indicate that this clade is monophyletic, congruent with previous reports (Molnár et al. 2002, Székely et al. 2009, 2015, Zhao et al. 2017), although several sub-clades were based on the precise location of the plasmodia. *M. xinyangensis* sp. nov. was found to cluster with *M. bhadrensis*, *M. kingchowensis* and *M. terengganuensis* within a sub-clade at the basal part of the tree. We therefore suspect that different infection sites drive the morphological differentiation of species in the lineage of *Myxobolus* that infect cyprinids intramuscularly. Our results also prove again that phylogenetic affinities of host and tissue tropism provide a stronger evolutionary signal than myxospore morphology (Eszterbauer 2004, Carriero et al. 2013). For example, 2 common carp muscle-infecting species, *M. artus* and *M. cyprini*, formed a sister relationship, even though they possess distinct spore body shapes (Chen & Ma 1998). However, to some extent, myxospore morphology can predict the phylogenetic relationships within the clade of cyprinid muscle-infecting species. For example, *M. bhadrensis*, *M. kingchowensis* and *M. terengganuensis*, which possess elongated ellipsoidal myxospores and tapered anterior spore ends, clustered together into an independent group. Among nominated *Myxobous* species that infect cyprinid muscle, few possess an oblate spore body, like *M. artus* and *M. yibinensis*, 2 common carp-infecting species. Obtaining molecular data on *M. yibinensis* to prove that it phylogenetically clusters with *M. artus* among the common carp muscle-infecting lineage, will further support the viewpoint of myxospore morphology-based phylogenetic correlation at a short evolutionary history (Liu et al. 2016). In the present analysis, however, *M. xinyangensis* sp. nov., which has an orbicular spore body, did not locate in the transitional position between the lineages with elongated ellipsoidal spore bodies and those with oblate spore bodies. This result can be partially explained by the species involved in the present phylogenetic analysis being positioned at wide evolutionary history. Furthermore, it can also not be ruled out that different myxospore shapes have evolved independently multiple times within the clade of *Myxobolus* species that infect cyprinid muscle (Liu et al. 2016).

M. haichengensis, which is the only species with available sequence data in GenBank among *Abbottina*-infecting myxosporeans, possesses a spore body shape (ellipsoidal vs. orbicular) and tissue tropism (gill filaments vs. trunk muscle) distinct from *M. xinyangensis* sp. nov. More sequence data are required to explore the phylogenetic relationships among *Abbottina*-infecting *Myxobolus* species.

Phylogenetic analysis also indicated the muscle tropism of *M. xinyangensis* sp. nov. All species clustering with it within an independent lineage infect the intracellularly muscle of cyprinids, although no histological analysis was conducted in the present work to determine the location of the plasmodia, as formalin-preserved samples were unavailable. *M. klamathellus* infects muscle rather than subcutaneously (Atkinson & Banner 2017), which presents symptoms of distinctly raised plasmodia outward, similar to *M. xinyangensis* sp. nov. The symmetrical distribution of plasmodia, as observed in *M. xinyangensis* sp. nov., is rarely reported among histozoic myxosporeans, although low infection prevalence may preclude this particular observation. The possible detrimental effects of infection by *M. xinyangensis* sp. nov. on the host warrant further study.

Acknowledgements. We appreciate the help of the local department of environmental protection in Xinyang City in collecting fish specimens. The study was financially supported by the Natural Science Foundation of China (31472296, 31772411).

LITERATURE CITED

Atkinson SD, Banner CR (2017) A novel myxosporean parasite *Myxobolus klamathellus* n. sp. (Cnidaria: Myxosporea) from native blue chub (*Gila coerulea*) in Klamath Lake, Oregon. Parasitol Res 116:299–302

Atkinson SD, Bartošová P, Whipps CM, Bartholomew JL (2015) Approaches for characterizing myxozoan species. In: Okamura B, Gruhl A, Bartholomew JL (2015) Myxozoan evolution, ecology and development. Springer International Publishing, Basel, p 111–121

Bartošová P, Fiala I, Hypša V (2009) Concatenated SSU and LSU rDNA data confirm the main evolutionary trends within myxosporeans (Myxozoa: Myxosporea) and provide an effective tool for their molecular phylogenetics. Mol Phylogenet Evol 53:81–93

Carriero MM, Adriano EA, Silva MRM, Ceccarelli PS, Maia AAM (2013) Molecular phylogeny of the *Myxobolus* and *Henneguya* genera with several new south American species. PLOS ONE 8:e73713

Chen QL, Ma CL (1998) Myxozoa: Myxosporea, Fauna Sinica. Science Press, Beijing (in Chinese)

Eiras JC, Molnár K, Lu YS (2005) Synopsis of the species of *Myxobolus* Bütschi, 1882 (Myxozoa: Myxosporea: Myxobolidae). Syst Parasitol 61:1–46

Eiras JC, Zhang JY, Molnár K (2014) Synopsis of the species of *Myxobolus* Bütschi, 1882 (Myxozoa: Myxosporea: Myxobolidae) described between 2005 and 2013. Syst Parasitol 88:11–36

Eszterbauer E (2004) Genetic relationships among gill-infecting *Myxobolus* species (Myxosporea) of cyprinids: molecular evidence of importance of tissue-specificity. Dis Aquat Org 58:35–40

Fiala I (2006) The phylogeny of Myxosporea (Myxozoa) based on small subunit ribosomal RNA gene analysis. Int J Parasitol 36:1521–1534

Fiala I, Bartošová P, Okamura B, Hartikainen H (2015) Adaptive radiation and evolution within the Myxozoa. In: Okamura B, Gruhl A, Bartholomew JL (2015) Myxozoan evolution, ecology and development. Springer International Publishing, Basel, p 69–84

Forró B, Eszterbauer E (2016) Correlation between host specificity and genetic diversity for the muscle-dwelling fish parasite *Myxobolus pseudodispar*: examples of myxozoan host-shift. Folia Parasitol 63:019

Guindon S, Dufayard JF, Lefort V, Anisimova M, Hordijk W, Gascuel O (2010) New algorithms and methods to estimate maximum-likelihood phylogenies: assessing the performance of PhyML 3.0. Syst Biol 59: 307–321

Guo Q, Huang M, Liu Y, Zhang X, Gu Z (2018) Morphological plasticity in *Myxobolus* Bütschi, 1882: a taxonomic dilemma case and renaming of a parasite species of the common carp. Parasit Vectors 11:399

Hall TA (1999) BioEdit: a user-friendly biological sequence alignment editor and analysis program for Windows 95/98/NT. Nucleic Acids Symp Ser 41:95–98

Hayashi K, Kin EJ, Onikura N (2013) Growth and habitat use of the Chinese false gudgeon, *Abbottina rivularis*, in an irrigation channel near the Ushizu River, northern Island, Japan. Ichthyol Res 60:218–226

Iwanowicz DD, Iwanowicz LR, Howerth EW, Schill WB, Blazer VS, Johnson RL (2013) Characterization of a new myxozoan species (Myxozoa: Myxobolidae: Myxosporea) in largescale stonerollers (*Campostoma oligolepis*) from the Mobile River basin (Alabama). J Parasitol 99:102–111

Kent ML, Watral VG, Whipps CM (2004) A digenean metacercaria (*Apophallus* sp.) and a myxozoan (*Myxobolus* sp.) associated with vertebral deformities in cyprinid fishes from the Willamette River, Oregon. J Aquat Anim Health 16:116–129

Li P, Zhao X, Xi BW, Xie J (2018) Supplemental description of *Myxobolus haichengensis*, 1958 (Myxozoa: Myxosporea) infecting the gills of *Abbottina rivularis* Basilewsky: morphological and molecular data. Acta Hydrobiol Sin 41:1–6

Liu XH, Batueva MD, Zhao YL, Zhang JY, Zhang QQ, Li TT, Li AH (2016) Morphological and molecular characterization of *Myxobolus pronini* n. sp. (Myxozoa: Myxobolidae) from the abdominal cavity and visceral serous membranes of the gibel carp *Carassius auratus gibelio* (Bloch) in Russia and China. Parasit Vectors 9:562

Lom J, Arthur JR (1989) A guideline for the preparation of species descriptions in Myxosporea. J Fish Dis 12: 151–156

Molnár K, Eszterbauer E, Székely C, Dán Á, Harrach B (2002) Morphological and molecular biological studies on intramuscular *Myxobolus* spp. of cyprinid fish. J Fish Dis 25:643–652

Ogawa K, Delgahapitiya KP, Furuta T, Wakabayashi H (1992) Histological studies on the host response to *Myxobolus artus* Akhmerov, 1960 (Myxozoa: Myxobolidae) infection in the skeletal muscle of carp, *Cyprinus carpio* L. J Fish Biol 41:363–371

Page RDM (1996) TREEVIEW: an application to display phylogenetic trees on personal computers. Comput Appl Biosci 12:357–358

Posada D (2008) jModelTest: phylogenetic model averaging. Mol Biol Evol 25:1253–1256

Ronquist F, Huelsenbeck JP (2003) MrBayes 3: Bayesian phylogenetic inference under mixed models. Bioinformatics 19:1572–1574

Székely C, Shaharom-Harrison F, Cech G, Ostoros G, Molnár K (2009) Myxozoan infections in fishes of the Tasik Kenyir Water Reservoir, Teregganu, Malaysia. Dis Aquat Org 83:37–48

Székely C, Cech G, Chaudhary A, Borzá R, Singh HS, Molnár K (2015) Myxozoan infections of the three Indian major carps in fish ponds around Meerut, UP, India, with descriptions of three new species, *Myxobolus basuhaldari* sp. n., *M. kalavatiae* sp. n. and *M. meerutensis* sp. n., and the redescription of *M. catlae* and *M. bhadrensis.* Parasitol Res 114:1301–1311

Tamura K, Stecher G, Peterson D, Filipski A, Kumar S (2013) MEGA6: Molecular Evolutionary Genetics Analysis version 6.0. Mol Biol Evol 30:2725–2729

Thompson JD, Gibson TJ, Plewniak F, Jeanmougin F, Higgins DG (1997) The CLUSTAL-X windows interface: flexible strategies for multiple sequence alignment aided by quality analysis tools. Nucleic Acids Res 25: 4876–4882

Whipps CM, Adlard RD, Bryant MS, Lester RJG, Findlay V,

Kent ML (2003) First record of three *Kudoa* species from eastern Australia: *Kudoa thyrsites* from mahi mahi (*Coryphaena hippurus*), *Kudoa amamiensis* and *Kudoa minithyrsites* n. sp. from sweeper (*Pempheris ypsilychnus*). J Eukaryot Microbiol 50:215–219

Zhai Y, Whipps CM, Gu Z, Guo Q, Wu Z, Wang H, Liu Y (2015) Intraspecific morphometric variation in myxosporeans. Folia Parasitol 63:011

Zhang JY, Wang JG, Li AH, Gong XN (2010) Infection of *Myxobolus turpisrotundus* sp. n. in allogynogenetic gibel carp, *Carassius auratus gibelio* (Bloch), with revision of *Myxobolus rotundus* (s.l.) Nemeczek reported from *C. auratus auratus* (L.). J Fish Dis 33:625–638

Zhao ZM, Liu XH, Zhao YL, Yuan S, Zhang JY (2017) Redescription and phylogenetic analysis based on 18S rDNA of *Myxobolus kingchowensis* (Myxozoa: Myxobolidae). Freshw Fish 47:79–85 (in Chinese with English abstract)

Appendix

Table A1. Fish collected in November 2017 during environmental assessment of the Huang River, Xinyang City (China). The species of interest (Chinese false gudgeon,infected with new myxosporean) is marked in **bold**

Species	Samples (n)
***Abbottina rivularis* Basilewsky, 1855**	51
Acheilognathus chankaensis Dybowski, 1872	16
Acheilognathus gracilis Nichols, 1926	55
Acheilognathus macropterus Bleeker, 1871	33
Channa argus Cantor, 1842	13
Chanodichthys dabryi Bleeker, 1871	17
Chanodichthys erythropterus Basilewsky, 1855	17
Chanodichthys mongolicus Basilewsky, 1855	43
Hemibarbus maculatus Bleeker, 1871	22
Hemiculter bleekeri Warpachowski, 1888	49
Macropodus ocellatus Cantor, 1842	58
Micropercops swinhonis Günther, 1873	19
Microphysogobio microstomus Yue, 1995	11
Misgurnus anguillicaudatus Cantor, 1842	29
Opsariichthys bidens Günther, 1873	71
Paramisgurnus dabryanus Dabry de Thiersant, 1872	9
Pseudobrama simony Bleeker, 1864	33
Pseudorasbora parva Temminck et Schlegel, 1846	62
Rhinogobius giurinus Rutter, 1897	38
Rhodeus ocellatus Kner, 1866	123
Sarcocheilichthys nigripinnis Günther, 1873	32
Saurogobio dabryi Bleeker, 1871	23
Squalidus argentatus Sauvage & Dabry de Thiersant, 1874	29
Tachysurus nitidus Sauvage & Dabry de Thiersant, 1874	11

Editorial responsibility: Dieter Steinhagen, Hannover, Germany

Submitted: August 23, 2018; Accepted: November 2, 2018
Proofs received from author(s): December 23, 2018